Minimum Mean Square Equalization in Cyclostationary and Stationary Interference–Analysis and Subscriber Line Calculations

Brent R. Petersen, *Student Member, IEEE*, and David D. Falconer, *Fellow, IEEE*

***Abstract*—We consider equalization in cyclostationary interference, a situation which occurs when similar neighboring digital communication systems cause interference. A new expression has been derived on the minimum mean square performance of a continuous-time infinite-length decision feedback equalizer in the presence of multiple cyclostationary interferers and additive white noise. This expression was calculated for a subscriber line system to show the performance improvements which can occur over the situation where the interference is stationary with the same power spectrum. Linear equalizer performance curves were also added to the comparisons. These results show two important techniques which can provide opportunities for improved equalizer performance by enhancing the cyclostationarity of the interference. The first is by decreasing the misalignment of the phases of the transceiver clocks in the central office transmitters. The second is by using transmitter pulse bandwidths which are wide relative to the symbol rate.**

I. Introduction

Communication channels where bandwidth efficiency is a prime concern often suffer from interference (crosstalk), a principal performance-limiting impairment in many communication systems. The type of cyclostationary interference [1] considered in this paper is crosstalk induced from similar neighboring digital communication systems. It occurs in transmission over digital subscriber lines [2], [3] and, under certain conditions, there may be significant variations of interference statistics at a receiver input [4]. We consider the performance of equalizers operating in such an environment, and discuss methods to enhance the cyclostationarity of the interference to improve that performance.

In this paper, a new minimum mean square error (MMSE) expression is derived on the performance of a continuous-time *infinite-length* decision feedback equalizer (DFE) in the presence of multiple cyclostationary interferers and additive white noise. As well, a new result is derived which states that every increase in bandwidth of size equal to the symbol rate may provide the flexibility to completely suppress an additional cyclostationary interferer.

The new DFE MMSE result is calculated for a high-speed digital subscriber line system and compared to the performance of a linear equalizer. Also, these two equalizers are compared to the situations where the power spectrum of the interference at the input to the receiver is the same, but stationary. The gains in cyclostationary versus stationary interference indicate the possibility for improved system performance by enhancing the cyclostationarity of the interference through providing *partial* alignment of the transmitter clock phases in the central office. We also demonstrate that wide transmitter pulse bandwidths, relative to the symbol rate, can allow significant performance improvements when the interference is cyclostationary. These results address maximum equalizer capability. Implementation issues such as timing jitter, adaptation, and coefficient precision have not been considered.

Our work, with preliminary results reported in [5]–[7], will now be put in context with previously published work. The ability to separate cyclostationary signals by exploiting their spectral correlation has been addressed in [8], [9] for a wide variety of conditions and applications. Specifically, in [10] the ability of a fractionally spaced linear equalizer to suppress cyclostationary interference is addressed through the theory of spectral correlation. We have only considered the case of linear and decision feedback equalization in cyclostationary interference, but in this framework we have given alternative insight into the reason for the gains in cyclostationary interference. This insight is given through the effects of relative transmitter pulse bandwidth in a generalized zero-forcing linear equalizer.

Expressions for the MMSE of a *finite-length* DFE in cyclostationary interference have been given in [11]–[14]. The expressions in [11], [12] appear in a more general

Manuscript received October 24, 1990; revised May 1, 1991. This paper was presented in part at the IEEE HDSL Workshop '90, Parsippany, NJ, March 28-29, 1990, and IEEE GLOBECOM '90, San Diego, CA, December 2-5, 1990. This research was supported by the Cable Telecommunications Research Institute (CTRI), the Telecommunications Research Institute of Ontario (TRIO), the Natural Sciences and Engineering Research Council (NSERC), and Carleton University.

The authors are with the Department of Systems and Computer Engineering, Carleton University, Ottawa, Ont., Canada K1S 5B6.

IEEE Log Number 9201627.

then two IFFT's, two

situation where a receiver has multiple inputs and is required to estimate the data from multiple streams. Many subtle relationships between single- and multiple-input receivers are described in [15].

The discovery of the benefit of relative transmitter bandwidth on the ability to suppress cyclostationary interference was reported in [5]–[7]; it was concurrently discovered and then reported in [9], [16], [17]. Calculations demonstrating this benefit in subscriber line interference were concurrently performed, as reported in [15].

In subscriber line systems, the issues of *completely aligned, completely misaligned*, and *randomly aligned* phases of the transmitter clocks in the central office have been addressed in [4], [13], [14], [18], [19].

Related work in the area of interference suppression has been published in [20]–[40].

II. System Model

The system model is shown in Fig. 1. In this model, a DFE estimates the transmitted data, $\{d_{n0}\}$, from the signal component at the input to the equalizer, $s(t)$, in the presence of additive white noise and cyclostationary interference, $v(t)$. The input to the equalizer is:

$$g(t) = \sum_{n=-\infty}^{\infty} d_{n0}\phi_0(t - nT) + n(t) + \sum_{i=1}^{L}\sum_{n=-\infty}^{\infty} d_{n_i}\phi_i(t - nT) \quad (1)$$

where the three terms are signal, noise, and crosstalk, respectively. T is the symbol period. L is the number of interferers.

The impulse response of the *overall* channel, $\phi_0(t)$, is the convolution of both the transmitter pulse and the channel impulse response. Similarly, the impulse response of the ith *overall* cochannel is the convolution of both the transmitter pulse and the ith interferer's impulse response. The complex baseband noise has a two-sided power spectrum N_0 and is white:

$$E[n(t)] = 0 \quad (2)$$

$$E[n(t_1)n^*(t_2)] = N_0\delta(t_1 - t_2). \quad (3)$$

$\delta(t)$ is the unit impulse and the symbol $*$ denotes complex conjugate transpose. The transpose will be relevant later, when dealing with matrices.

Throughout this paper, the data are complex and satisfy the following:

$$E[d_{n_i}] = 0 \quad (4)$$

$$E[d_{n_i}d^*_{mk}] = \delta_{i-k}\delta_{n-m} \quad (5)$$

$$\delta_k = \begin{cases} 1, & k = 0 \\ 0, & k \neq 0 \end{cases} \quad (6)$$

where $E[\cdot]$ will always denote expectation over the data and noise. The data are uncorrelated with the noise.

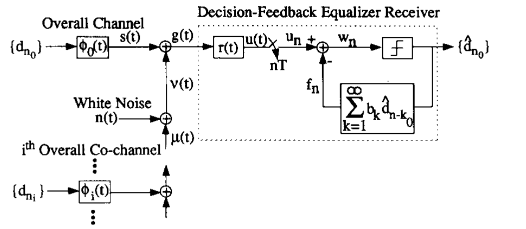

Fig. 1. System model: Cyclostationary interference and decision-feedback equalizer receiver.

III. Decision Feedback Equalizer Analysis

A. MMSE Expression Assuming Cyclostationary Interference

The performance criterion that is used to analyze the DFE is the mean square error (MSE):

$$\epsilon_d = E[|w_n - d_{n0}|^2] \quad (7)$$

where w_n is the output of the DFE, shown in Fig. 1. We assume correct decisions ($\hat{d}_{n0} = d_{n0}$) throughout this paper. The MSE was chosen for two reasons. First, it makes analysis of the equalizer tractable. Second, it is minimized in efficient adaptive equalizer implementations [41].

At any point in the following development, the impulse responses of the interferers can be set to zero to get the familiar situation of a linear channel with additive white noise. The following analysis is a generalization of elements of [42], [43], which are based on a linear channel with additive white noise.

Given a known overall channel and overall cochannels, the problem is to find the impulse response of the forward filter of the DFE, $r(t)$, and the coefficients of the feedback filter, $\{b_k | k = 1, 2, 3, \cdots\}$, to minimize the MSE, ϵ_d. Knowledge of the overall channel and overall cochannels is needed to determine the minimum MSE expression, but adaptive equalizers do not necessarily require such knowledge. Since correct decisions are assumed and the equalizer may have an infinite number of tap coefficients, the derivation is for a lower bound on the MSE of an implementation, but the result should closely approximate the performance of an implementation with a sufficiently large number of taps, ignoring error propagation.

Consider Fig. 1. The MSE may be rewritten as:

$$\epsilon_d = E[w_n w_n^*] - E[d_{n0}w_n^*] - E[d^*_{n0}w_n] + E[d_{n0}d^*_{n0}] \quad (8)$$

where

$$w_n = u_n - f_n \quad (9)$$

the output of the feedback filter is:

$$f_n = \sum_{k=1}^{\infty} b_k d_{(n-k)0} \quad (10)$$

and the sampled forward filter output is:

$$u_n = \int_{-\infty}^{\infty} g(\tau)r(nT - \tau)\,d\tau. \quad (11)$$

In the development of the DFE where the data is uncorrelated and the only channel impairment is additive white noise, to minimize the MSE requires the coefficients of the feedback filter, $\{b_k \mid k = 1, 2, 3, \cdots\}$, be set equal to the samples of the equalized channel [42]. By the calculus of variations [44], it can be shown that this is true in cyclostationary interference as well:

$$b_k = \int_{-\infty}^{\infty} \phi_0(kT - \tau)\, r(\tau)\, d\tau; \qquad k = 1, 2, 3, \cdots. \tag{12}$$

This was expected since setting the coefficients this way makes the postcursor intersymbol interference (ISI) zero. The coefficients could be set after $r(t)$ has been determined, but the minimum MSE expression can be determined without explicitly finding them.

Substituting w_n, f_n, u_n, and b_k from (9)–(12) into (8) and evaluating the expectations, the MSE becomes:

$$\begin{aligned}\epsilon_d = &\int_{-\infty}^{\infty}\int_{-\infty}^{\infty} k_d(t, \tau)\, r^*(t) r(\tau)\, d\tau\, dt \\ &- \int_{-\infty}^{\infty} \phi_0^*(-t) r^*(t)\, dt \\ &- \int_{-\infty}^{\infty} \phi_0(-t) r(t)\, dt + 1\end{aligned} \tag{13}$$

where the Hermitian kernel is:

$$k_d(t, \tau) = N_0 \delta(t - \tau) + \sum_{m=-\infty}^{0} \phi_0(mT - \tau)\phi_0^*(mT - t) \tag{14}$$

$$+ \sum_{i=1}^{L} \sum_{m=-\infty}^{\infty} \phi_i(mT - \tau)\phi_i^*(mT - t). \tag{15}$$

The problem is to find $r(t)$ which minimizes the MSE given in (13), and by the calculus of variations [43], [44] the optimal function for $r(t)$, call it $r_o(t)$, satisfies the following integral equation:

$$\int_{-\infty}^{\infty} k_d(t, \tau) r_o(\tau)\, d\tau = \phi_0^*(-t). \tag{16}$$

By substituting (16) into (13), the minimum MSE (MMSE), ϵ_{d_o}, can be rewritten in terms of the optimal forward filter:

$$\epsilon_{d_o} = 1 - \int_{-\infty}^{\infty} \phi_0(-t) r_o(t)\, dt \tag{17}$$

$$= 1 - \int_{-\infty}^{\infty} \Phi_0(f) R_o(f)\, df \tag{18}$$

where $R_o(f)$ and $\Phi_i(f)$ are the Fourier transforms of $r_o(t)$ and $\phi_i(t)$, respectively.

Expanding the integral in (16) and grouping all integrals over $d\tau$ into constants which are not functions of t and rearranging gives the form of the optimal forward filter (provided $N_0 \neq 0$):

$$r_o(t) = \sum_{n=-\infty}^{0} a_{n_0}\phi_0^*(nT - t) + \sum_{i=1}^{L}\sum_{n=-\infty}^{\infty} a_{n_i}\phi_i^*(nT - t) \tag{19}$$

where

$$a_{n_i} = \begin{cases} -\dfrac{1}{N_0} u_{n_0}; & i = 0; n < 0 \\ \dfrac{1}{N_0}(1 - u_{0_0}); & i = 0; n = 0 \\ -\dfrac{1}{N} u_{n_i}; & i = 1, 2, 3, \cdots, L; \forall n \end{cases} \tag{20}$$

and

$$u_{n_i} = \int_{-\infty}^{\infty} \phi_i(nT - \tau) r_o(\tau)\, d\tau. \tag{21}$$

The form of (19) indicates that the optimal forward filter can be interpreted as a bank of filters matched to the individual $\{\phi_i(t) \mid i = 0, 1, 2, \cdots, L\}$ followed by synchronous filters (T-spaced tapped delay lines), as shown in Fig. 2. The synchronous filter following the matched filter $\phi_0^*(-t)$ is anticausal while the synchronous filters following the filters matched to the interferers are two-sided. Note that for the case where all the interferers are zero, Fig. 2 reverts to the familiar form of a matched filter followed by an anticausal synchronous equalizer which minimizes the MSE due to the precursor ISI [42].

An important note about this equalizer is that it is *time-invariant.* The time invariance occurs because the MSE is minimized only at symbol-rate samples, and because the output of the channel is wide-sense stationary when sampled at the symbol frequency. To properly verify that the equalizer is time-invariant, the development should have been started from a time-variant point of view, but the excess notation would make the explanation unnecessarily complex. Note that the classical MMSE equalizer for a data signal without crosstalk is also time-invariant even though the data signal is cyclostationary.

The integral equation (16) remains to be solved for $r_o(t)$ and the details of this part of the solution have been previously given in [5], [7]. Using $r_o(t)$, (17)–(18), and the analysis in [42], this gives us the new fundamental result for DFE MMSE which is summarized here. When the overall channel and cochannels, $\{\Phi_i(f) \mid i = 0, 1, 2, \cdots, L\}$, are strictly bandlimited to $K/(2T)$ where K is a positive integer, then the MMSE of a continuous-time infinite-length DFE in cyclostationary interference and additive white noise is:

$$\epsilon_{d_o} = e^{-\langle \ln(1 + M_T(f)) \rangle} \tag{22}$$

where

$$\langle \cdot \rangle = T \int_{-(1/(2T))}^{+(1/(2T))} [\cdot]\, df \tag{23}$$

then two IFFT's,

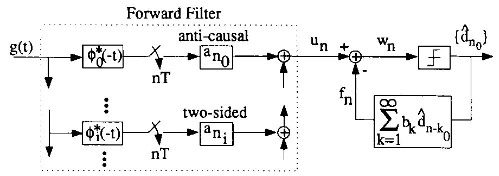

Fig. 2. Form of the MMSE decision feedback equalizer.

$$M_T(f) = \frac{1}{T}\,\Phi_0^*(f)\,W^{-1}(f)\,\Phi_0(f); \qquad -\frac{1}{2T} \le f \le \frac{1}{2T}. \tag{24}$$

$\Phi_0(f)$ is a column vector with $(2K - 1)$ rows:

$$\Phi_i(f) = \left[\Phi_i\left(f - \frac{K-1}{T}\right)\ \Phi_i\left(f - \frac{K-2}{T}\right) \cdots \Phi_i\left(f + \frac{K-1}{T}\right)\right]^*. \tag{25}$$

$W(f)$ is a $(2K - 1) \times (2K - 1)$ matrix:

$$W(f) = N_0 I_{2K-1} + \frac{1}{T}\sum_{i=1}^{L} \Phi_i(f)\,\Phi_i^*(f) \tag{26}$$

and I_{2K-1} is an identity matrix of the order $2K - 1$. Refinements of the notation of the MMSE expression, beyond [7], were based on similar work for a linear equalizer [16], [45].

Consider the following qualitative description of the behavior of the MMSE DFE. The forward filter of the DFE acts to cause the sampled equalized channel to be at or near zero at the sampling points before the time origin and at or near unity at the time origin [42], [46]. The sampled equalized channel to the right of the time origin is not relevant to the forward filter because the feedback part of the DFE subtracts off the remaining ISI. This is the same as the additive white noise case with no interferers. However, in the presence of interferers, the forward filter also acts to make the sampled equalized cochannel at or near zero for all sampling points. Thus, the MSE consists of four terms due to: bias in the estimate of the data [47], precursor ISI, crosstalk, and noise, respectively. The MMSE DFE minimizes the sum of the four terms.

B. MMSE Expression Assuming Stationary Interference

In Fig. 1, the power spectrum of the interference, $v(t)$, averaged over one symbol period is:

$$S_{vv}(f) = N_0 + \frac{1}{T}\sum_{i=1}^{L} |\Phi_i(f)|^2. \tag{27}$$

$S_{vv}(f)$ is the result of the sum of the independent power spectrums of noise and multiple baseband linearly modulated signals [8], [47]. If the interference shown in Fig. 1 is replaced with a stationary noise process having the same power spectrum as (27), then the MMSE DFE in stationary interference can be determined by whitening the noise in the channel [42], [48]. Such an MMSE expression is not new, but it is partially described because the numerical calculations in Section VI have more emphasis on comparing the MMSE of the cyclostationary case relative to this stationary case.

IV. Linear Equalizer Performance

A. MMSE Expression Assuming Cyclostationary Interference

In addition to considering decision feedback equalizers, we have included linear equalizers in our subscriber line calculations in Section VI. The expression for the MMSE of a linear equalizer in cyclostationary interference is well known [5], [10], [15], [16], [21], [23], [27], [28], [32], [33], [45] and will only be stated:

$$\epsilon_{l_0} = \left\langle \frac{1}{1 + M_T(f)} \right\rangle \tag{28}$$

where $M_T(f)$ is defined in the same manner as for the DFE (24).

B. MMSE Expression Assuming Stationary Interference

Linear equalizer MMSE expressions in stationary interference with power spectrum given by (27) can be derived by whitening the noise and using the analyses in [43], [48], [49].

V. Bandwidth Considerations

Interestingly, one can show that the MMSE expressions in cyclostationary interference will reduce to the same expressions as in the stationary interference case if the interferers $\{\Phi_i(f) \mid i = 1, 2, 3, \cdots, L\}$ are strictly bandlimited to $1/(2T)$. This is a result of the cyclostationary interference becoming wide-sense stationary as the bandwidth of the interferers is reduced below $1/(2T)$ [1]. Hence, the bandwidth beyond $1/(2T)$ is crucial in providing an opportunity to exploit the cyclostationarity of the interference. The discussion in this section is intended to give insight into the amount of bandwidth beyond $1/(2T)$ which is beneficial for enhancing the cyclostationarity of the interference and for improving the equalizer's interference-suppression capability. A result will be derived which states that relatively wider bandwidths in the overall channel and overall cochannels, $\{\Phi_i(f) \mid i = 0, 1, 2, \cdots, L\}$, with respect to the symbol rate, provide the flexibility to suppress larger number of cyclostationary interferers.

For the simplicity of description, a generalized zero-forcing linear equalizer will be analyzed, similar to previous work [50], except that now we consider the effect of bandwidth. Delete the feedback loop in Fig. 1 and let the equalized channels and cochannels be:

$$H_i(f) = \Phi_i(f)R(f); \qquad i = 0, 1, 2, \cdots, L. \tag{29}$$

In the frequency domain, the condition for zero ISI and zero cochannel interference is [50]:

$$\frac{1}{T}\sum_{l=-\infty}^{\infty} H_i\left(f+\frac{l}{T}\right) = \delta_i; \qquad i = 0, 1, 2, \cdots, L. \tag{30}$$

In (30), the case of $i = 0$ corresponds to the condition for zero ISI. Substituting $H_i(f)$ from (29) into (30) gives:

$$\frac{1}{T}\sum_{l=-\infty}^{\infty} \Phi_i\left(f+\frac{l}{T}\right)R\left(f+\frac{l}{T}\right) = \delta_i;$$
$$i = 0, 1, 2, \cdots, L. \tag{31}$$

Equation (31) represents $L + 1$ equations over $\{i = 0, 1, 2, \cdots, L\}$ where the values of $R(f)$ are unknown. If the $\{\Phi_i(f) \mid i = 0, 1, 2, \cdots, L\}$ are strictly bandlimited to $K/(2T)$, where K is a positive integer, then in the frequency range $-1/(2T) < f < 1/(2T)$ there will be up to K unknowns. Other frequency ranges would produce similar independent equations. The system of equations in (31) is shown in matrix form for the case where K is odd:

$$\begin{bmatrix} \Phi_0\left(f+\frac{K-1}{2T}\right) & \Phi_0\left(f+\frac{K-3}{2T}\right) & \cdots & \Phi_0\left(f-\frac{K-1}{2T}\right) \\ \Phi_1\left(f+\frac{K-1}{2T}\right) & \Phi_1\left(f+\frac{K-3}{2T}\right) & \cdots & \Phi_1\left(f-\frac{K-1}{2T}\right) \\ \vdots & \vdots & \ddots & \vdots \\ \Phi_L\left(f+\frac{K-1}{2T}\right) & \Phi_L\left(f+\frac{K-3}{2T}\right) & \cdots & \Phi_L\left(f-\frac{K-1}{2T}\right) \end{bmatrix} \begin{bmatrix} R\left(f+\frac{K-1}{2T}\right) \\ R\left(f+\frac{K-3}{2T}\right) \\ \vdots \\ R\left(f-\frac{K-1}{2T}\right) \end{bmatrix} = \begin{bmatrix} T \\ 0 \\ \vdots \\ 0 \end{bmatrix}. \tag{32}$$

The case where K is even produces an equivalent derivation.

With the absence of further knowledge about the values of the overall channel and overall cochannels, it is difficult to proceed. However, if those values were chosen randomly, then (32) will likely have a solution when the number of equations is less than or equal to the number of unknowns. To state this result another way, let $N = L + 1$ where N is the number of independent data streams. Then, (32) will likely have a solution when the number of independent data streams is less than or equal to the number representing the bandwidth:

$$N \leq K. \tag{33}$$

Even if (33) is satisfied, the system of equations in (32) will *not* have a solution in pathological cases, such as the case when the overall channels and cochannels have identical frequency responses. Define $\boldsymbol{p}_0$ to be the row vector in (32) formed from $\{\Phi_0(f)\}$ and define $\{\boldsymbol{p}_1, \boldsymbol{p}_2, \cdots, \boldsymbol{p}_L\}$ to be the set of row vectors formed from $\{\Phi_i(f) \mid i = 1, 2, 3, \cdots, L\}$, respectively. Since the linear equalizer is required to estimate only the single data stream corresponding to $\boldsymbol{p}_0$, then (32) will have at least one solution if $\boldsymbol{p}_0$ is linearly independent of $\{\boldsymbol{p}_1, \boldsymbol{p}_2, \cdots, \boldsymbol{p}_L\}$ [15].

The generalized zero-forcing linear equalizer will exist if (32) has solutions for all frequencies, except for possibly one small subset of frequencies, provided that the MSE still consists of only one finite component due to channel noise.

In summary, (33) states: *Every increase in bandwidth of size equal to the symbol rate may provide the flexibility to completely suppress an additional interferer by means of linear equalization.* Without further knowledge about the values of the overall channel and overall cochannels, the emphasis of this analysis remains on its insight into the *flexibility* that relatively wide bandwidths may provide to *MMSE* linear and decision feedback equalizers when they trade off suppression of ISI, cochannel interference, and noise. In the application of Section VI, the overall channel and overall channels take on specific values. This permits further discussion about the benefits of relatively wide bandwidths.

VI. Subscriber Line Calculations

To compare the MMSE performance of linear and decision feedback equalizers in cyclostationary interference versus stationary interference, a number of subscriber-line system calculations were performed. These evaluations further quantify the benefits of aligning the transmitter clock phases in the central office, and the benefits of relatively wide bandwidths.

The overall channel and overall cochannels are convolutions of the transmitter pulse, $p(t)$, with the channel and cochannels, $c_i(t)$:

$$\phi_i(t) = p(t) * c_i(t); \qquad i = 0, 1, 2, \cdots, L. \tag{34}$$

The frequency response of the Butterworth transmitter pulse is shown in Fig. 3; the magnitudes are in linear scale and the phase is in radians. The symbol rate, $1/T$, is 400 kHz. The parameter B is the maximum baseband bandwidth, expressed in units relative to the symbol rate which we call *symbol frequencies.* The pulse is shown for $B = 1$ symbol frequency, which means that it is strictly bandlimited to $1/T$ with a 3 dB cutoff frequency at $1/(2T)$. If B were increased, it would mean that the pulse would be linearly stretched in frequency relative to the symbol rate and the magnitude of the pulse would be scaled down by an appropriate amount to maintain a constant transmitter power. For example, if B were 1.5 sym-

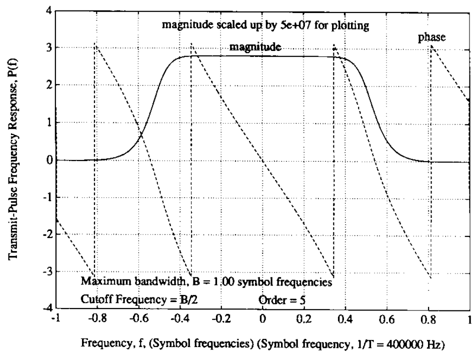

Fig. 3. Transmitter-pulse frequency response–Butterworth filter.

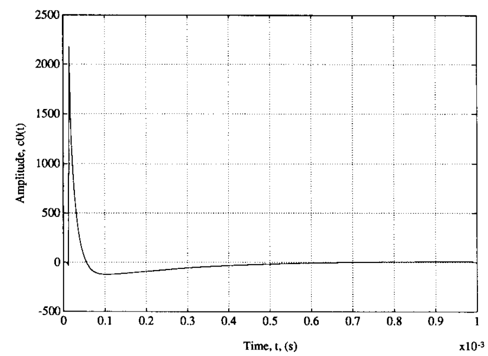

Fig. 4. Channel impulse response–9000 feet of 26 AWG wire.

bol frequencies, then the pulse would be bandlimited to $3/(2T)$, would have a 3 dB cutoff frequency at $3/(4T)$, and would have a magnitude smaller than the example shown in Fig. 3. When $B = 0.5$ symbol frequencies, this pulse has the same maximum bandwidth as a raised cosine pulse [47] with 0% excess bandwidth. Similarly, $B = 1$ symbol frequency corresponds to 100% excess bandwidth. The effective bandwidth will be less than the maximum bandwidth due to the presence of white noise in the channel. Note also that the pulse *shape* was not varied since its effect on performance, in this application, is expected to be less significant than that of the relative pulse bandwidth. A similar effect was observed for stationary interference in [51]. However, in other applications it may be economical to design the shapes of the wide-bandwidth transmitter pulses to achieve improved interference suppression capability.

The channel is 9000 feet of 26-gauge wire. This is one of the worst-case lines considered for high-speed digital subscriber line transmission. The impulse response of the channel, $c_0(t)$, is shown in Fig. 4.

The frequency response of one cochannel, $C_1(f)$, is shown in Fig. 5; the magnitudes are in linear scale and the phase is in radians. This response was obtained from processing near-end crosstalk (NEXT) coupling measurements on a 50-pair telephone cable [18]. To exploit the cyclostationarity of the interference, phase information is essential. Also shown is a commonly used worst-case stationary NEXT model, which includes only magnitude information [2], [3].

Using the cochannels obtained from measurements, the corresponding overall cochannels were obtained by convolution with the transmitter pulse and the results are shown in Fig. 6, spread out in time for better visibility. The number of interferers shown is $L = 6$. Notice that they are very similar in shape, but differing in amplitude. They were obtained from measurements [18] which occurred on a single cable with all crosstalk coupling paths having similar geometries. These measurements are the most realistic results available to us, in the absence of any other accessible NEXT measurements incorporating phase information of real subscriber lines. Fig. 6 introduces two

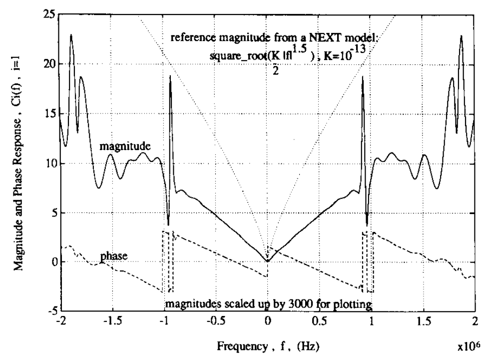

Fig. 5. One cochannel frequency response–obtained from near-end crosstalk coupling measurements.

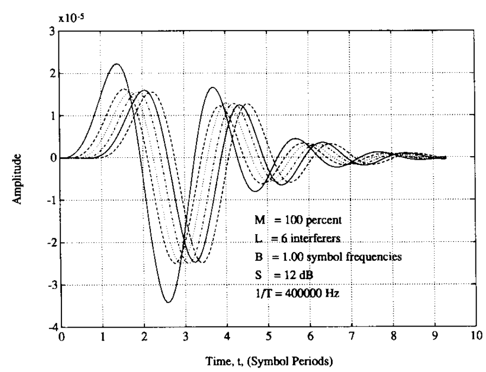

Fig. 6. Overall cochannels' impulse responses, $\{\phi_i(t) | i = 1, 2, 3, \cdots, L\}$.

parameters. The parameter S indicates that the powers of the interferers were scaled up by a design safety factor of 12 dB [3]. The parameter M was used to study the effects of aligning the phases of the clocks at the central office, not the clocks at customer end where the NEXT is less severe. M is the percent misalignment over one symbol period. Stated another way, the beginnings of the impulse responses of the interferers are uniformly distributed over M% of a symbol period. When M is 0%, the interferers are perfectly aligned in phase and the interference has the largest amount of cyclostationarity. When M is 100%, the interference has the least amount of cyclostationarity. Note that M was not obtained from measurements but introduced as a parameter in the calculations.

Referring to Fig. 1, the signal power is:

$$P_S = \frac{1}{T}\int_0^T E[|s(t)|^2]\,dt \tag{35}$$

the interferer power is:

$$P_I = \frac{1}{T}\int_0^T E[|\mu(t)|^2]\,dt \tag{36}$$

and the bandlimited complex noise power is:

$$P_N = N_0\left(2\,\frac{B}{T}\right) \tag{37}$$

where $\{\Phi_i(f)\,|\,i = 0, 1, 2, \cdots, L\}$ are strictly bandlimited to B/T due to the transmitter pulse. The powers in (35)–(37) were calculated for the increasing numbers of interferers present and the results are shown in Fig. 7. The noise power was arbitrarily set to be 15 dB below the power of the strongest interferer.

The ratio of the maximum-to-minimum interferer power, in dB, over a symbol period was calculated for values of the interference misalignment M ranging from 0 to 100% and the results are plotted in Fig. 8. As expected, the power variation decreases as the interference misalignment is increased, indicating that the interference becomes more stationary. For these particular interferer impulse responses, the power variation does not go completely to zero as M approaches 100%, mainly because the interferers have different amplitudes. The power variation does not appear to be closely related to the *gains* achievable by fractionally spaced equalizers in exploiting the cyclostationarity of the interference. Instead, the power variation is more closely related to the MMSE *variations* that could be experienced by a *symbol-spaced equalizer* in cyclostationary interference [13], [14].

The equations for the DFE MMSE (22) and linear equalizer MMSE (28) were evaluated along with the MMSE performance in the previously described stationary interference model. The MMSE for the four cases of interference and equalizer types are shown in Fig. 9 versus D, the relative time shift of the signal with respect to the interference over one symbol period. The value of D is determined by the random phase of the transmitter clock at the customer end. The interference misalignment was set to 0% to demonstrate how large the differences between cyclostationary and stationary interference can become. As expected, the performance in stationary interference is unchanged with D. However, the performance in cyclostationary interference varies with D, and the value which causes the performance improvement in cyclostationary interference over stationary interference to be the smallest is 0.72 symbol periods. Even at the worst-case alignment of the interference with respect to the signal, the performance in cyclostationary interference is better than in stationary interference. Note that a bandwidth of $B = 1$ symbol frequency implicitly means that $T/2$-spaced equalizers are needed to approach these MMSE results. In contrast, a T-spaced equalizer which is restricted to sampling the received signal once per symbol interval would have a performance in cyclostationary interference that is worse than in stationary interference, for

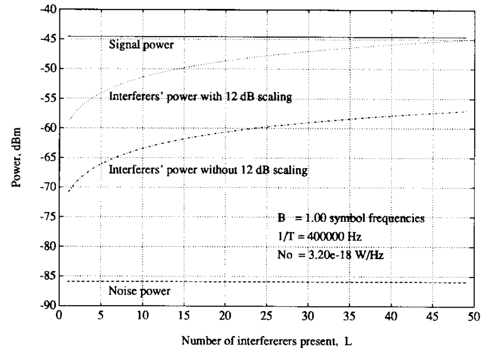

Fig. 7. Signal, interference, and noise powers versus number of interferers.

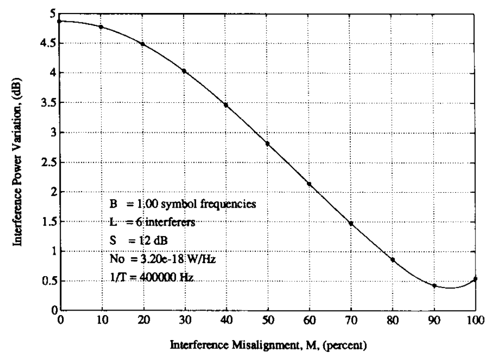

Fig. 8. Interference power variation in a symbol period versus interference misalignment.

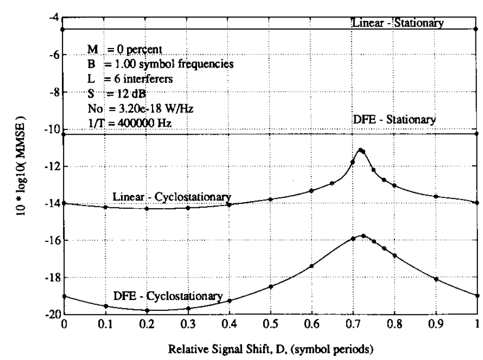

Fig. 9. Linear and decision feedback equalizer MMSE versus relative signal shift.

this channel. Similar results for *finite* numbers of tap coefficients were reported in [13], [14].

Using the worst value of the relative signal shift, $D = 0.72$ symbol periods, the four MMSE cases are plotted versus the interference misalignment to explore the effects of aligning the clock phases of the interference at the central office (see Fig. 10). The DFE MMSE in cyclostationary interference reduces to only 3 dB better than the stationary case when the interference misalignment is increased to 10%. For the linear equalizer, the corresponding value of M is 15%. These results are based on a transmitter pulse with $B = 1$ symbol frequency. The discussion of Section V suggested that larger relative bandwidths provide a greater opportunity to suppress interference.

Consider the point of 3 dB improvement in Fig. 10. The values of the interference misalignment M near this point are used in Fig. 11 where MMSE is plotted versus the relative pulse bandwidth B. As the bandwidth increases, it demonstrates that the gains due to exploiting the cyclostationarity increase significantly. At the largest bandwidth of B equal to 1.5 symbol frequencies, the improvement is 10 dB for the DFE in cyclostationary versus stationary interference. The MMSE improvements increase with increasing bandwidth, but they reach diminishing returns.

Using a wider bandwidth pulse with $B = 1.5$ symbol frequencies [bandlimited to $3/(2T)$] and the worst possible relative signal shift of $D = 0.72$ symbol periods, the MMSE expressions versus the interference misalignment M were recalculated and are shown in Fig. 12. The performance improvements using the relatively wide bandwidth pulse are significant. The DFE MMSE in cyclostationary interference maintains at least a 3 dB improvement over the stationary case, while the interference misalignment is increased up to 40%. The relatively wide pulse gives larger gains, and permits a higher interference misalignment for the same performance improvement. Note that, with a bandwidth of $B = 1.5$ symbol frequencies, $T/3$-spaced equalizers would be needed for implementation.

The discussion of Section V suggested that bandwidths where $B = 1$ symbol frequency may provide the flexibility to suppress all ISI and one cochannel interferer, or many synchronized cochannel interferers with nearly the same interfering pulse shape. When the bandwidth is increased to $B = 1.5$ symbol frequencies, there may be enough flexibility to suppress all ISI and two cochannel interferers. However, note that the increased relative bandwidth does not mean that the MMSE equalizers eliminate one more particular interferer, but instead the increased bandwidths mean that the equalizers have increased flexibility to find a better MMSE solution.

The effect of interference misalignment on the MMSE for two different pulse bandwidths were shown in Figs. 10 and 12 for the case of $L = 6$ interferers. These calculations were repeated for the worst-case situation of $L = 49$ interferers, using crosstalk measurements obtained from [18], and the results are shown in Figs. 13 and 14. With the relatively wide bandwidth pulse used for Fig. 14, the DFE MMSE improvements in cyclostationary over stationary interference vary from 14 to 0 dB as the interference misalignment is increased from 0 to 100%, with the point of 3 dB margin occurring at an interference misalignment of near 45%.

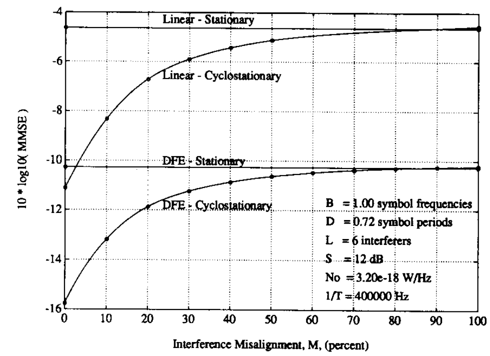

Fig. 10. Linear and decision feedback equalizer MMSE versus interference misalignment.

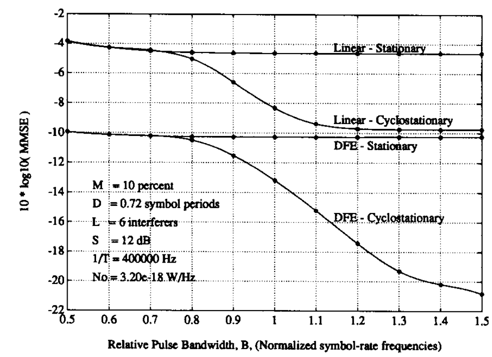

Fig. 11. Linear and decision feedback equalizer MMSE versus transmitter-pulse bandwidth.

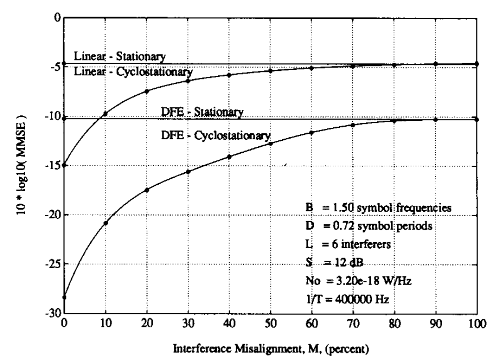

Fig. 12. Linear and decision feedback equalizer MMSE versus interference misalignment-wider transmitter-pulse bandwidth.

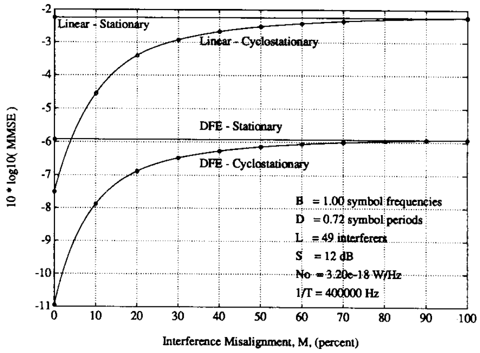

Fig. 13. Linear and decision feedback equalizer MMSE versus interference misalignment—49 interferers.

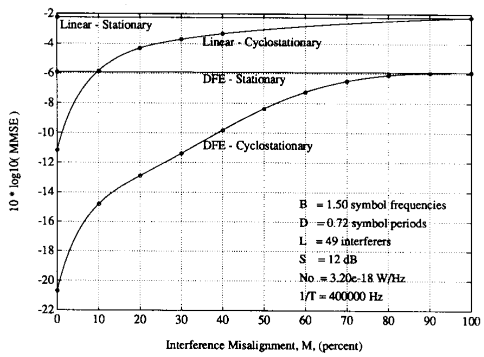

Fig. 14. Linear and decision feedback equalizer MMSE versus interference misalignment-wider transmitter-pulse bandwidth and 49 interferers.

Naturally, exploiting the gains in cyclostationary interference does not occur without some cost. It would be necessary to provide sufficient, but not perfect, alignment of the clock phases in the central office and, with relative pulse bandwidths of beyond $B = 0.5$ symbol frequencies, fractionally spaced equalizers are required for implementation.

VII. Conclusions

We have presented a new MMSE expression for a continuous-time infinite-length DFE in cyclostationary interference and additive white noise. We have also presented a new result which states that every increase in bandwidth of size equal to the symbol rate may provide the flexibility to completely suppress an additional interferer, depending upon the application.

Through MMSE calculations of high-speed digital subscriber line systems, we compared the DFE and linear equalizer performances in cyclostationary and stationary interference. We have attempted to quantify the performance gains which can occur due to aligning the phases of the transceiver clocks at the central office. These results are intended to motivate the telephone operating companies to perform similar evaluations with measurements on subscriber lines of more realistic geometries. As demonstrated here, even if perfect clock-phase alignment does not occur, there are gains by exploiting the cyclostationarity of the interference.

In subscriber line calculations, which included the effect of white noise, we demonstrated that relatively wide bandwidth transmitter pulses provide the flexibility to fractionally spaced equalizers for significant performance improvements in cyclostationary interference.

To achieve these gains requires *conventional* adaptive equalizer implementations having sufficient numbers of taps, small enough tap spacing, and tap coefficients with sufficient precision [13], [14], [16].

Finally, it is worth noting that these transmitter and equalizer design considerations, which are relevant to high-speed digital subscriber line transmission, may also be relevant in other interference-limited environments.

Acknowledgment

The authors are sincerely grateful to M. L. Honig of Bell Communications Research and G. D. Golden of AT&T Bell Laboratories for showing them prepublication research [15], [16], [45], and for giving them helpful suggestions about their work. They also thank the anonymous reviewers for their valuable comments.

References

[1] W. A. Gardner and L. E. Franks, "Characterization of cyclostationary random processes," *IEEE Trans. Inform. Theory*, vol. IT-21, no. 1, pp. 4-14, Jan. 1975.

[2] J. W. Lechleider, "Loop transmission aspects of ISDN basic access," *IEEE J. Select. Areas Commun.*, vol. SAC-4, no. 8, pp. 1294-1301, Nov. 1986.

[3] —, "High bit rate digital subscriber lines—A review of HDSL progress," this issue, pp. 769-784.

[4] J. C. Campbell, A. J. Gibbs, and B. M. Smith, "The cyclostationary nature of crosstalk interference from digital signals in multipair cable-Part I: Fundamentals and Part II: Applications and further results," *IEEE Trans. Commun.*, vol. COM-31, no. 5, pp. 629-649, May 1983.

[5] B. R. Petersen and D. D. Falconer, "Equalization in cyclostationary interference," Tech. Rep. SCE 90-01, Dept. Syst. Comput. Eng., Carleton Univ., Ottawa, Ont., Canada, Jan. 1990.

[6] —, "Equalization bounds in cyclostationary subscriber-loop interference," presented at the IEEE High-Speed Digital Subscriber Lines Workshop, Parsippany, NJ, Mar. 28-29, 1990.

[7] —, "Exploiting cyclostationary subscriber-loop interference by equalization," in *Conf. Rec. IEEE GLOBECOM'90*, San Diego, CA, Dec. 2-5, 1990, vol. 2, pp. 1156-1160.

[8] W. A. Gardner, *Introduction to Random Processes with Applications to Signals and Systems.* New York: McGraw-Hill, 1990.

[9] —, "Exploitation of spectral redundancy in cyclostationary signals," *IEEE Signal Process. Mag.*, vol. 8, no. 2, pp. 14-36, Apr. 1991.

[10] W. A. Gardner and W. A. Brown, "Frequency-shift filtering theory for adaptive co-channel interference removal," in *Proc. Twenty-Third Asilomar Conf. Signals, Syst., Comput.*, Pacific Grove, CA, Oct. 30-Nov. 1, 1989, pp. 562-567.

[11] D. G. Messerschmitt, L. C. Barbosa, and T. D. Howell, "A study of sampling detectors for magnetic recording," Tech. Rep. DJ 4081 (45459) (declassified July 7, 1987), IBM Almaden Research Center, San Jose, CA, July 16, 1984.

[12] M. Kavehrad and J. Salz, "Cross-polarization cancellation and equalization in digital transmission over dually polarized multipath fading channels," *AT&T Tech. J.*, vol. 64, no. 10, pp. 2211-2245, Dec. 1985.

[13] M. Abdulrahman and D. D. Falconer, "Crosstalk suppression by DFE

then two IFFT's, two

on digital subscriber loops," in *Proc. Canad. Conf. Elect. Comput. Eng.*, Ottawa, Ont., Canada, Sept. 4-6, 1990, vol. 2, pp. 78.2.1-78.2.4.

[14] —, "Cyclostationary crosstalk suppression by decision feedback equalization on digital subscriber loops," to appear in *IEEE Trans. Commun.*

[15] P. M. Crespo, M. L. Honig, and K. Steiglitz, "Suppression of near- and far-end crosstalk by linear pre and post-filtering," to appear in *IEEE Trans. Commun.*

[16] G. D. Golden, "Cancellation of synchronous cyclostationary interference (SCI) using fractionally spaced equalizers," invited seminar, Dept. Syst. Comput. Eng., Carleton Univ., Ottawa, Ont., Canada, Mar. 7, 1990.

[17] W. A. Gardner and S. Venkataraman, "Performance of optimum and adaptive frequency-shift filters for cochannel interference and fading," in *Proc. Twenty-Fourth Asilomar Conf. Signals, Syst., Comput.*, Pacific Grove, CA, Nov. 5-7, 1990.

[18] A. Fung, L. S. Lee, and D. D. Falconer, "A facility for near end crosstalk measurements on ISDN subscriber loops," in *Conf. Rec. IEEE GLOBECOM'89*, Dallas, TX, Nov. 27-30, 1989, vol. 3, pp. 1592-1596.

[19] V. Joshi and D. D. Falconer, "Sequence estimation techniques for digital subscriber loop transmission with crosstalk interference," *IEEE Trans. Commun.*, vol. 38, no. 9, pp. 1367-1374, Sept. 1990.

[20] D. J. Harrison, "Adaptive equalization for channels with crosstalk," Master's Thesis, Fac. Eng., Carleton Univ., Ottawa, Ont., Canada, Sept. 1969.

[21] A. R. Kaye and D. A. George, "Transmission of multiplexed PAM signals over multiple channel and diversity systems," *IEEE Trans. Commun.*, vol. COM-18, no. 5, pp. 520-526, Oct. 1970.

[22] L. H. Brandenburg and A. D. Wyner, "Capacity of the Gaussian channel with memory: The multivariate case," *Bell Syst. Tech. J.*, vol. 53, no. 5, pp. 745-778, May/June 1974.

[23] W. van Etten, "An optimum linear receiver for multiple channel digital transmission systems," *IEEE Trans. Commun.*, vol. COM-23, no. 8, pp. 828-834, Aug. 1975.

[24] —, "Maximum likelihood receiver for multiple channel transmission systems," *IEEE Trans. Commun.*, vol. COM-24, no. 2, pp. 276-283, Feb. 1976.

[25] P. Monsen, "MMSE equalization of interference on fading diversity channels," *IEEE Trans. Commun.*, vol. COM-32, no. 1, pp. 5-12, Jan. 1984.

[26] J. H. Winters, "Optimum combining in digital mobile radio with cochannel interference," *IEEE J. Select. Areas Commun.*, vol. SAC-2, no. 4, pp. 528-539, July 1984.

[27] N. Amitay and J. Salz, "Linear equalization theory in digital data transmission over dually polarized fading radio channels," *AT&T Tech. J.*, vol. 63, no. 10, pp. 2215-2259, Dec. 1984.

[28] J. Salz, "Digital transmission over cross-coupled linear channels," *AT&T Tech. J.*, vol. 64, no. 6, pp. 1147-1159, July/Aug. 1985.

[29] M. Kavehrad, "Baseband cross-polarization interference cancellation for M-quadrature amplitude-modulated signals over multipath fading radio channels," *AT&T Tech. J.*, vol. 64, no. 8, pp. 1913-1926, Oct. 1985.

[30] S. Verdú, "Optimum multiuser asymptotic efficiency," *IEEE Trans. Commun.*, vol. COM-34, no. 9, pp. 890-897, Sept. 1986.

[31] H. V. Poor and S. Verdú, "Single-user detectors for multiuser channels," *IEEE Trans. Commun.*, vol. 36, no. 1, pp. 50-60, Jan. 1988.

[32] E. Biglieri, M. Elia, and L. LoPresti, "The optimal linear receiving filter for digital transmission over nonlinear channels," *IEEE Trans. Inform. Theory*, vol. 35, no. 3, pp. 620-625, May 1989.

[33] P. M. Crespo, M. L. Honig, and K. Steiglitz, "Optimization of pre- and post-filters in the presence of near- and far-end crosstalk," in *Conf. Rec. IEEE ICC 89*, Boston, MA, June 11-14, 1989, vol. 1, pp. 541-547.

[34] L. W. Lechleider, "The feasibility of using adaptive transmitters to suppress crosstalk," in *Conf. Rec. IEEE ICC'89*, Boston, MA, June 11-14, 1989, pp. 548-551.

[35] M. Uesugi, K. Honma, and K. Tsubaki, "Adaptive equalization in TDMA digital mobile radio," in *Conf. Rec. IEEE GLOBECOM'89*, Dallas, TX, Nov. 27-30, 1989, vol. 1, pp. 95-101.

[36] M. L. Honig, K. Steiglitz, and B. Gopinath, "Multichannel signal processing for data communications in the presence of crosstalk," *IEEE Trans. Commun.*, vol. 38, no. 4, pp. 551-558, Apr. 1990.

[37] P. Niger and P. Vandamme, "Performance of equalization techniques in a radio environment," in *Conf. Rec. IEEE ICC'90*, Atlanta, GA, Apr. 16-19, 1990, vol. 2, pp. 473-477.

[38] M. L. Dukić, Z. D. Stojanović, and I. S. Stojanović, "Performance of direct-sequence spread-spectrum receiver using decision feedback and transversal filters for combatting narrowband interference," *IEEE J. Select. Areas Commun.*, vol. 8, no. 5, pp. 907-914, June 1990.

[39] C. L. Despins, D. D. Falconer, and S. A. Mahmoud, "Coding and optimum baseband combining for wideband TDMA indoor wireless channels," in *Conf. Rec. IEEE GLOBECOM'90*, San Diego, CA, Dec. 2-5, 1990, vol. 3, pp. 1832-1837.

[40] —, "Coding and optimum baseband combining for wideband TDMA indoor wireless channels," *Can. Elec. Eng. J.*, vol. 16, no. 2, pp. 53-62, Apr. 1991.

[41] M. L. Honig and D. G. Messerschmitt, *Adaptive Filters: Structures, Algorithms and Applications.* Boston, MA: Kluwer, 1984.

[42] J. Salz, "Optimum mean-square decision feedback equalization," *Bell Syst. Tech. J.*, vol. 52, no. 8, pp. 1341-1373, Oct. 1973.

[43] R. D. Gitlin and S. B. Weinstein, "Fractionally-spaced equalization: An improved digital transversal filter," *Bell Syst. Tech. J.*, vol. 60, no. 2, pp. 275-296, Jan. 1981.

[44] A. E. Danese, *Advanced Calculus: An Introduction to Applied Mathematics.* Boston, MA: Allyn and Bacon, 1965.

[45] G. D. Golden, AT&T Bell Laboratories, Holmdel, NJ, private commun., Jan. 1991.

[46] R. Price, "Nonlinearly feedback-equalized PAM versus capacity for noisy filter channels," in *Conf. Rec. IEEE ICC'72*, Philadelphia, PA, June 19-21, 1972, vol. 1, pp. 22.12-22.16.

[47] J. G. Proakis, *Digital Communications.* New York: McGraw-Hill, 1983.

[48] T. Kailath, "The innovations approach to detection and estimation theory," *Proc. IEEE*, vol. 58, no. 5, pp. 680-695, May 1970.

[49] R. W. Lucky, J. Salz, and E. J. Weldon, *Principles of Data Communication.* New York: McGraw-Hill, 1968.

[50] D. A. Shnidman, "A generalized Nyquist criterion and an optimum linear receiver for a pulse modulation system," *Bell Syst. Tech. J.*, vol. 46, pp. 2163-2177, Nov. 1967.

[51] W. F. McGee, "Coding, equalization and feedback of digital cable pair signals," *Can. Elec. Eng. J.*, vol. 7, no. 1, pp. 3-8, Jan. 1982.

Brent R. Petersen (S'85) was born in Whitehorse, Yukon Territory, Canada on March 25, 1962. He received the B.Eng. degree in electrical engineering from Carleton University, Ottawa, Ont., Canada in 1985, and the M.A.Sc. degree in electrical engineering from the University of Waterloo, Ontario, Canada in 1987.

He returned to Carleton University in 1987, where he is presently working towards the Ph.D. degree in electrical engineering. He has worked at Northern Telecom Electronics Ltd. in automatic test program generation for VLSI circuits, at Bell Northern Research in scan testing of VLSI circuits, and at the Defense Research Establishment Ottawa in the navigation group. His research interests include digital communications, digital signal processing, and computer-aided design of integrated circuits.

David D. Falconer (M'68-SM'83-F'86), for a photograph and biography, see this issue, p. 875.